ASCE

Evaluation of Steel Fiber–Reinforced Sprayed Concrete by Energy Absorption Tests

Alan Renato Estrada Cáceres[1]; Sergio Henrique Pialarissi Cavalaro[2]; and Antonio Domingues de Figueiredo[3]

Abstract: Steel fiber–reinforced sprayed concrete (SFRSC) is widely used for ground support in underground works. The panel test, as in EN 14488-5, is one of the most common procedures for the quality control of the energy absorption capacity of SFRSC. The test entails the use of large equipment to manipulate and characterize heavy specimens that cannot be easily extracted from a structure in case a direct assessment of the material in place is needed. Alternative procedures, such as the Barcelona test (BCN), have been used to assess the energy absorption of cast fiber–reinforced concrete in smaller-scale cylindrical specimens that can be extracted from a structure and are considerably less demanding in terms of equipment and payload. The objective of this study is to evaluate the use of the BCN as a substitution of the traditional square panel test to assess the energy absorption of SFRSC. Both tests were conducted in parallel in combination with the quantification of the incorporated fiber content through an inductive test. Hence, the analysis reflects the actual control conditions of the SFRSC under the influence of spraying. Results indicate a possible reliable correlation between the BCN and panel test if the cracked area is considered. Different sizes of cores were tested to understand the influence of this parameter in energy absorption by the BCN test. The reduction of specimen size demands an increase in the number of determinations per batch to ensure representative results. The study suggests that the BCN can be considered a viable method of evaluating the energy absorption of SFRSC in cores extracted from test panels or actual tunnel linings. **DOI: 10.1061/(ASCE)MT.1943-5533.0003865.**

Author keywords: Steel fiber; Sprayed concrete; Barcelona test (BCN); Square panel test; Inductive test; Energy absorption.

Introduction

Steel fibers are used in sprayed concrete to provide post-cracking reinforcement to enhance toughnesss avoiding the typical brittle behavior of this material (Bernard and Thomas 2020) and enhancing dynamic mechanical properties (Chen et al. 2020). Steel fiber–reinforced sprayed concrete (SFRSC) is widely used in a variety of applications including, construction of slope stabilization, excavation support, structure recovery, refractory lining, tunnel lining, mining operations, etc. (Pfeuffer and Kusterle 2001; Cengiz and Turanli 2004; Bernard 2008; Ginouse and Jolin 2015; Galobardes et al. 2019; Liu et al. 2020). One of the most traditional applications of SFRSC is tunnel lining by the New Austrian Tunneling Method (NATM). Specifications [e.g., EFNARC 1996; EN 14487-1 (CEN 2005)] classify the SFRSC in this application according to the material energy absorption capacity measured in flexural tests of square panels. The results obtained in the test are used both in the design and systematic quality control. For instance, the Australian Institute of Concrete (Concrete Institute of Australia 2010) takes the energy absorption class measured in the square panel test and the rock formation as input parameters for the tunnel lining design.

The square panel test is currently defined by the standard EN 14488-5 (CEN 2006). Modifications in the specimen shape and test procedure proposed to facilitate execution and improve the results include the three-point bending test of square panels with a notch (EFNARC 2011) and round panel test [ASTM C1550-12 (ASTM 2012)]. Previous studies have addressed the correlation between different panel shapes (Bernard 2002; Myren and Bjøntegaard 2010) and proposed the use of even larger round panels for increased reliability (Bernard 2013). These methods, however, entail a significant degree of complexity and imply the use of sizeable testing equipment and specimens challenging to produce and manipulate. Possibly the main drawback of these tests lays in the impossibility to extract flat specimens from the curved lining in case a direct verification is needed. Differences in the boundary conditions during the execution of the structure and the panel can lead to different material consolidation and fiber rebound that could compromise the representativeness of the test results (Figueiredo and Helene 1993; Austin et al. 1997; Jolin 1999; Armelin and Banthia 2002; Kaufmann et al. 2013).

Figueiredo (1997), Bernard (2002), and Myren and Bjøntegaard (2010) highlight a significant variability in the panel test results. Papworth (2002) suggests that the non-uniform moulding procedure of panels can lead to inconsistencies in the test results. The production of sufficiently flat, regular specimens is one of the major challenges towards ensuring adequate contact with the support during the test, which might have a significant influence on the results (Bernard 2002). Visual observations reveal that frictional forces between the panel and the supports have a direct impact on the energy absorbed (Myren and Bjøntegaard 2010).

Alternative procedures, such as the Barcelona test (BCN) defined in UNE 83515 (AENOR 2010), have been used to assess

[1]Ph.D. Candidate, Dept. of Civil Construction Engineering, Polytechnic School, Univ. of São Paulo, Caixa Postal 61548, CEP 05508-900, Sao Paulo, Brazil (corresponding author). ORCID: https://orcid.org/0000-0001-5708-4004. Email: alan.estrada@usp.br

[2]Full Professor, School of Architecture, Building and Civil Engineering, Loughborough Univ., Loughborough, Leics LE113TU, UK. Email: S.Cavalaro@lboro.ac.uk

[3]Associate Professor, Dept. of Civil Construction Engineering, Polytechnic School, Univ. of São Paulo, Caixa Postal 61548, CEP 05508-900, Sao Paulo, Brazil. ORCID: https://orcid.org/0000-0003-4658-3355. Email: antonio.figueiredo@usp.br

Note. This manuscript was submitted on September 4, 2020; approved on January 29, 2021; published online on July 15, 2021. Discussion period open until December 15, 2021; separate discussions must be submitted for individual papers. This paper is part of the ***Journal of Materials in Civil Engineering***, © ASCE, ISSN 0899-1561.

the energy absorption in smaller-scale cast fiber-reinforced concrete (FRC) cylindrical specimens, that can be extracted from the structure and are considerably less demanding in terms of equipment and payload. In the BCN, cylinder punches concentrically placed above and below the specimen produce internal tensile stresses that induce the crack formation and opening. The UNE 83515 (AENOR 2010) specifies that the increment in specimen perimenter due to cracking should be measured with a circumferential extensometer.

Pujadas et al. (2013) demonstrate that the increment in perimeter can be calculated from the vertical displacement of the press, thus avoiding the use of the expensive circumferential extensometer not found in most quality control laboratories (Monte et al. 2014). The use of this simplified BCN has proved to be an adequate method for the FRC quality control (Simão et al. 2019). Its application for the assessment of the energy absorption of sprayed FRC and the potential correlation of the results with those obtained through traditional panel tests still lack further research.

Carmona et al. (2020) correlated the absorbed energy of macrosyntetic fiber reinforced sprayed concrete by means of the BCN test, using a circumferential extensometer, and the square panel test, obtaining good correlation of results. However, the correlation equations were obtained using cast concrete, which differs from sprayed concrete due to the spraying conditions. It was proved by Banthia et al. (1994) and Leung et al. (2005) that there is no perfect parallelism between the mechanical properties of cast and sprayed FRC in the same dosage.

In order to know the actual fiber content incorporated in the structure, a new methodology was developed, the inductive test (Torrents et al. 2012; Cavalaro et al. 2015). This test can be applied to cylindrical cores (Cavalaro et al. 2016) and has been previously used to quantify the fiber content in SFRSC cores (Silva et al. 2015; Galobardes et al. 2019). Still few studies have been developed considering this method in the evaluation of SFRSC.

The objective of this study is to clarify these issues and to evaluate the potential use and implications of the simplified BCN together with the inductive test in substitution of the traditional square panel test. The analysis reflects the real control conditions of the material under the influence of the spraying process. The energy absorption results of two sizes of cylinders tested through the BCN test were correlated with those obtained from the square panel test. Findings derived from this study might support alternative approaches for the quality control of sprayed FRC and enable more straightforward verification of both properties of already built linings and the spraying process conditions.

Methodology

Spraying Process

The mix composition of the concrete is shown in Table 1. The dry materials chosen for the experimental program are commonly used in tunnel linings production in the region of Sao Paulo, Brazil. A polyfunctional admixture based on lignosulphonate solution, a superplasticiser based on a polycarboxilate solution and a hydration stabiliser composed by a sucrose derivate were added to the composition to ensure adequate fresh state properties. The concrete was supplied in a concrete mixer truck.

The steel fiber used as reinforcement was classified as type C-II according to the Brazilian standard ABNT NBR 15530 (ABNT 2007), with 39 mm length with and aspect ratio of 25 [Fig. 1(a)]. This fiber with low aspect-ratio was selected in order to evaluate one of the most critical conditions of SFRSC. Fibers were added in 3 nominal contents (approximately 30, 60, and 90 kg/m^3) directly to the truck and mixed thoroughly before the concrete was placed in the pump CP 10-SU [Fig. 1(b)]. This equipment has a nominal capacity of spraying of 10 cubic meters per hour and is mainly applied in tunnel linings with cross-sectional area bigger than 40 m^2. The mixture was sprayed on wood moulds positioned at 20° to the vertical axis [Fig. 1(c)]. An accelerator admixture based on aluminium sulphate solution (approximately 24 kg/m^3) was used to ensure adequate material consolidation over the surface. The wet spraying process replicates that typically found in ground support applications.

Table 1. Concrete mix composition

Materials	Content (kg/m^3)
Cement (70% CEM I 52.5R and 30% blast-furnace slag)	400
Fine quartz sand (0–0.6 mm)	574
Crushed granitic sand (0–4.8 mm)	315
Crushed granite coarse aggregate (4.8–12.5 mm)	840
Water	200
Polyfunctional admixture	1.44
Superplasticiser	0.84
Hydration stabilizer	1.12

Once the production of a test panel series related to lower fiber content was completed, the volume of the remaining concrete was estimated and an extra amount of fiber was added to the concrete truck to achieve the intermediate fiber content. Once the intermediate fiber content test panels were cast, the remaining volume of concrete was again estimated and a last portion of fibers was added to the mix to produce the last series of test panels with the highest fiber content. Notice that ensuring the exact fiber contents of 30, 60, and 90 kg/m^3 is not essential for conducting this study as the actual average content was assessed in all cylindrical cores. These nominal fiber contents were chosen aiming to cover the three levels of energy absorption (500, 700, 1,000 J) considered in the EN 14487-1 standard, according to the methodology of Figueiredo (1997). The average sprayed concrete compressive strength for each nominal fiber content at 5 months was: 39.1, 38.5, and 37.2 MPa, respectively. The results meet the compressive strength requirements for permanent sprayed concrete (30 MPa or greater) (Thomas 2020).

The sprayed specimens were square pyramidal truncated panels of two sizes: small panels of 600 × 600 mm at the base, 800 × 800 mm at the top, and thickness of 100 mm; and large panels of 600 × 600 mm at the base, 1,000 × 1,000 mm at the top, and thickness 200 mm. 4 small panels and 1 large panel were sprayed with each nominal fiber content. An additional small panel was produced for the nominal contents of 60 and 90 kg/m^3.

Square Panel Test–EN 14488-5

At the age of 5 months since production, 14 small panels (4 for the concrete with the lowest nominal fiber content and 5 for each of the others) were tested according to the EN 14488-5 using a 200 tf Shimadzu machine, as shown in Fig. 2. A square metal plate (100 × 100 × 5 mm) was cast with mortar at the central part of the panels to mitigate irregularities in the spraying surface and ensure uniform load application. The surface of the panel in contact with the mould was positioned on a square steel support, leaving a free square area in the central part of 500 mm side. In some cases, steel thin sheets had to be placed on the edges to obtain a continuous contact between the test panels and the support. The tests were performed at a constant rate of 1 ± 0.1 mm/min. LVDTs were used to measure the displacement, positioned at a yoke fixed at the

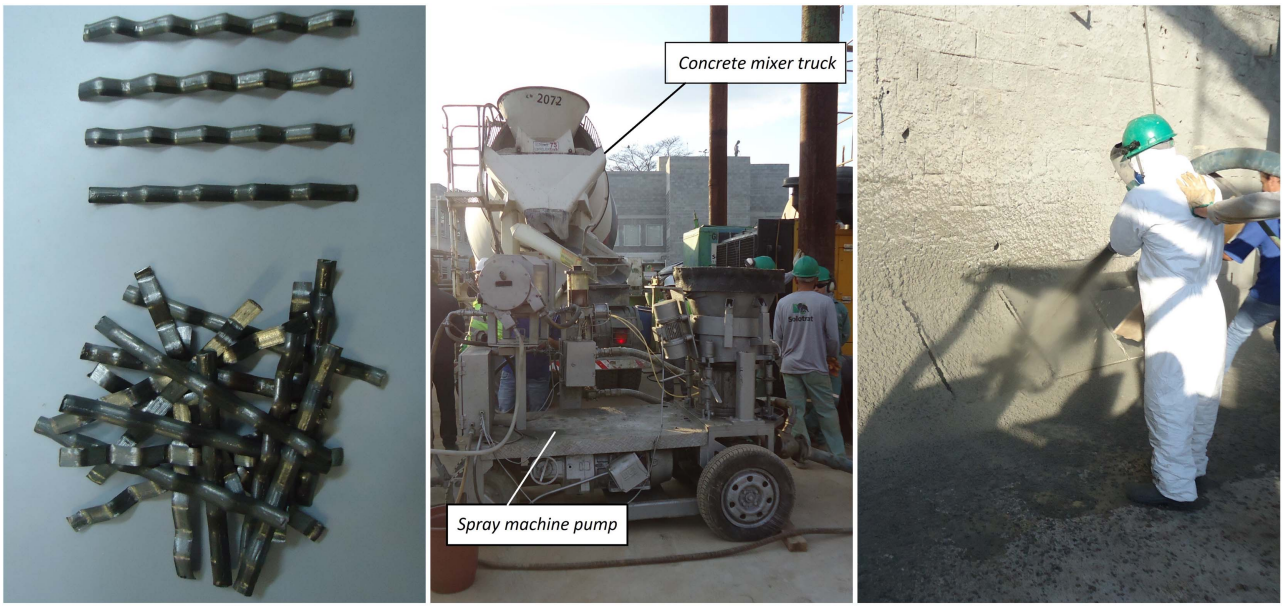

Fig. 1. (a) Steel fiber used; (b) concrete truck and pump; and (c) spraying process.

Fig. 2. Square panel test according to EN 14488-5.

frame, in order to reduce external deformations. An analysis of the absorbed energy in Joules was made by calculating the area under the load-displacement curve obtained in the tests.

Extraction of Cores

Cylindrical cores were extracted from the panels using a diamond crown cup saw. Large cylinders of nominal size of Ø150 × 150 mm (diameter × height) were extracted from large panels [Fig. 3(a)]. Small cylinders of Ø100 × 100 mm were extracted from small panels after the flexural test [Fig. 3(b)]. This process was performed carefully, avoiding extracting cylinders from cracked regions. The rough end of the core was cut to ensure the same height across all specimens. The specimens were used in the tests described in the next items.

Barcelona Test

The test was performed on a 200 tf Shimadzu universal machine following the procedure proposed by Pujadas et al. (2013). 18 large cylinders (Ø150 × 150 mm) and 83 small ones (Ø100 × 100 mm) were tested at 5 and 7 months since production, respectively. The large cylinders are dived in 6 per panel from each fiber content; the small cylinders are divided in 23 from the concrete with lower fiber content (6 per panel minus 1 cylinder that was discarded), 30 from the concrete with the intermediate and higher fiber content, respectively (6 per panel). A constant piston displacement rate of 0.5 ± 0.05 mm/min was used in all cases. The cylinders were kept in the same position, that is, the face in contact with the mould at the base of the test machine. The punching load was applied using Ø25 × 20 mm steel cylinders for the small specimens and Ø37.5 × 30 mm for the large ones to comply with the specimen-metallic punch diameter ration of 1/4 defined in UNE 83515 (AENOR 2010). The steel cylinders were concentrically placed on the upper and lower faces of the specimen (Fig. 4). The absorbed energy was calculated as the area under the load-displacement curve in Joules.

Inductive Test

The fiber content was determined by the inductive test (Torrents et al. 2012; Cavalaro et al. 2015). Initially, calibration procedure was performed with styrofoam cylinders, three of Ø100 × 100 mm (785.40 cm^3) and three of Ø150 × 150 mm (2,650.72 cm^3) in which fibers were inserted manually in a random manner to achieve contents of 30, 60, and 90 kg/m^3. The inductance change measured can be used to calculate the inductance coefficients for the fiber used, as described in Cavalaro et al. (2016). Fig. 5 shows

(a) (b)

Fig. 3. Cylinder extraction from (a) large panels; and (b) small panels.

Fig. 4. Barcelona test (BCN).

the correlations between the fiber content placed in the styrofoam cylinders and the summed inductance variation ΔL_T measured in the 3 orthogonal axes. A linear relationship is both cylinder sizes with intersect 0 (condition without fiber) and a slope β equal to 0.0109 and 0.0103 for large and small cylinders, respectively. The similar β despite the variation on specimens sizes highlights the accuracy of the method.

Eq. (1) gives the fiber content (C_f) within the cores in kg/m^3, depending on slop coefficient β, the total inductance variation (ΔL_T) in mH and volume (V) in m^3. Since the inductance change produced by concrete and styrofoam is negligible in comparison to that induced by the steel fibers, the same equation and coefficients apply to the cores extracted in the experimental programme

$$C_f = \beta \times \frac{\Delta L_T}{V} \tag{1}$$

The inductive test was perfomed on the same cylinders used in the BCN test, before undergoing this test. The notations used to present the results are M1, M2, and M3, corresponding to the concretes with nominal fiber contents of 30, 60, and 90 kg/m^3, respectively. The letters L and S are added at the beginning of the notation refer to the large and small cylinders, respectively. For example, L_M3 refers to the large cylinders with 90 kg/m^3 nominal fiber content.

Results and Analysis

Inductive Test

Table 2 shows the fiber content assessed in the large and small cylinders, including mean values, standard deviation (SD), COV, number of specimens of sample (N), maximum values (max), and minimum values (min). The average fiber content found in specimens L_M1 is 46.98 ± 2.19 kg/m^3, which is considerably higher than the nominal fiber content of 30 kg/m^3. The L_M2 and L_M3 cylinders have similar fiber contents of (79.60 ± 5.96 and 76.85 ± 8.58 kg/m^3, respectively) despite the difference in the nominal fiber content (60 and 90 kg/m^3, respectively).

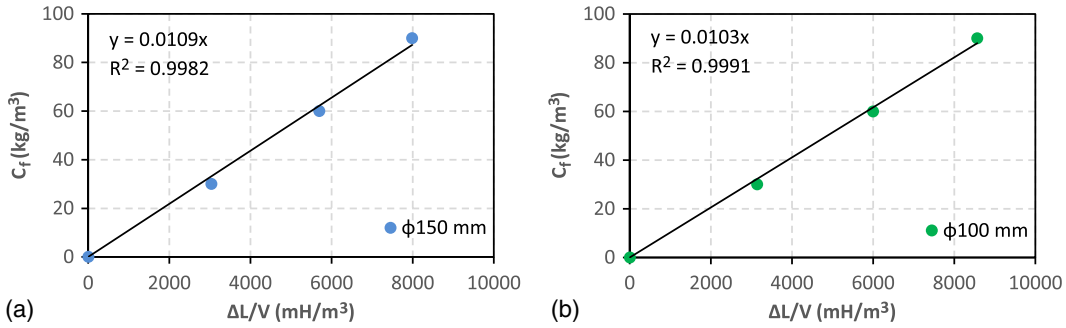

Fig. 5. (a) Inductive method calibration in styrofoam cylinders of Ø150 × 150 mm; and (b) Ø100 × 100 mm.

Table 2. Fiber content (C_f) in kilograms per cubic meter of extracted cylinders

Statistical parameter	Cylinders of Ø150 × 150 mm			Cylinders of Ø100 × 100 mm		
	L_M1	L_M2	L_M3	S_M1	S_M2	S_M3
Mean	46.98	79.60	76.85	33.88	63.02	74.92
SD	2.19	5.96	8.58	4.32	7.31	10.24
COV (%)	4.67	7.48	11.16	12.75	11.60	13.66
N	6	6	6	23	30	30
Max	49.45	89.38	86.46	47.05	82.27	93.48
Min	44.28	71.23	63.55	24.66	51.80	54.02

Small cylinders S_M1 and S_M2 with the lower and intermediate fiber contents (33.88 ± 4.32 and 63.02±7.31 kg/m^3, respectively) show results close to the nominal contents (30 and 60 kg/m^3, respectively), while small cylinders S_M3 with the highest fiber content (74.92 ± 10.24 kg/m^3) display results lower than the nominal value (90 kg/m^3). Small cylinders presented a high COV associated to the smaller total weight of fiber within the specimen in comparison with the total weight found in larger cylinders. This can be intensified by the fact that a fiber with low aspect ratio was used, which implies a more significant weight variation due to the changes in the number of fibers in the sample.

For subsequent analysis, the average fiber content measured for the cylinders, determined by the inductive test, will be used. The fiber contents obtained in the small cylinders also correspond to the small panels from which they were extracted, and will be used in the evaluation of the square panel test EN 14488-5.

Square Panel Test–EN 14488-5

Fig. 6 shows the mean load (P) and absorbed energy (E) versus displacement (δ) curves. Table 3 summarizes the energy absorption for a displacement of 25 mm (E_{25}), panel thickness (h), and number of cracks (N_c) after the test, considering the major and minor cracks. The mean values, SD, COV, N, and max and min values are also provided.

Both fiber content and panel thickness influence the energy absorption results in Table 3. The panels with higher fiber content (74.92 kg/m^3) and higher thickness (121.25 mm) show the highest average energy absorption value (976.18 ± 174.51 J), followed by the panels with fiber contents of 63.02 and 33.88 kg/m^3, which have energy absorption values of 578.18 ± 47.22 and 488.85 ± 50.38 J, respectively. The cracking pattern was generally 4 cross-shaped major cracks in panels with fiber contents of 33.88 and 63.02 kg/m^3 [Fig. 7(a)]. The number of cracks tends to increase for the content of 74.92 kg/m^3. For example, the panel with the highest energy absorption value of 1,176.07 J presented five major and two minor cracks [Fig. 7(b)]. Panels with lower and medium fiber contents show a smaller number of cracks because a simple biaxial flexion occurs. As fiber content increases, the degree of redundancy in the test increases (Myren and Bjøntegaard 2010; Salehian et al. 2014; Juhasz et al. 2017); this, in addition to the friction forces in the supports, causes punching shear failure (Carmona et al. 2020); therefore, the number of cracks increases. Cracking close to the edge of the panel could be highly affected by the support. Future studies focusing on that matter are needed.

The influence of the panel thicknesses on the absorbed energy was also reported by Bjøntegaard (2009), Myren and Bjøntegaard (2010), and Sandbakk (2011). A correction factor, based on the study of Thorenfeldt (2006) *apud* Myren and Bjøntegaard (2010)

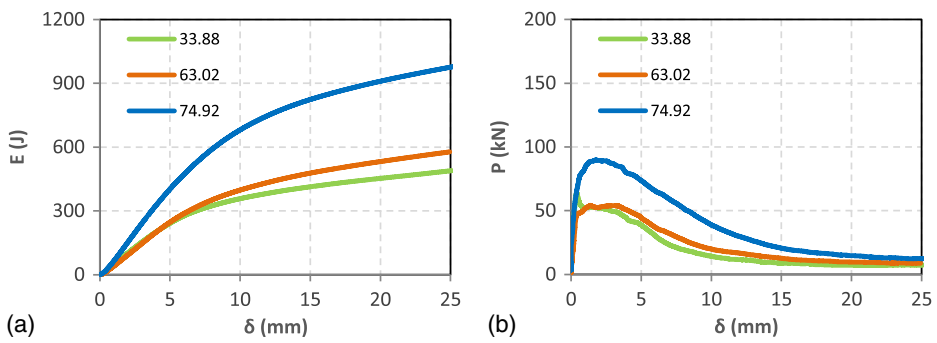

Fig. 6. Average curves of (a) load; and (b) energy absorption versus displacement, based on EN 14488-5 test on small panels with fiber contents of 33.88, 63.02, and 74.92 kg/m^3.

Table 3. Absorbed energy in 25 mm (E_{25}) in Joules for smaller panels according to EN 14488-5, panel thickness (h) in millimeters, number of cracks on panels (N_c) after being tested, factor of correction (k), modified displacement (Δ) in millimeters, corrected absorbed energy (E_c) in Joules

Statistical parameter	E_{25}	h	N_c	k	$\Delta = 25 \cdot k$	$E_c = K \cdot E_\Delta$
			Panels ($C_f = 33.88$ kg/m^3)			
Mean	488.85	117.61	3.75	0.85	21.28	397.85
SD	50.38	4.02	0.50	0.03	0.72	30.31
COV (%)	10.31	3.42	13.33	3.37	3.37	7.62
N	4	4	4	4	4	4
Max	538.51	122.99	4.00	0.88	21.93	422.11
Min	424.94	113.98	3.00	0.81	20.33	354.17
			Panels ($C_f = 63.02$ kg/m^3)			
Mean	578.18	112.05	4.40	0.89	22.31	494.18
SD	47.22	1.51	0.55	0.01	0.30	37.12
COV (%)	8.17	1.35	12.45	1.34	1.34	7.51
N	5	5	5	5	5	5
Max	629.05	114.29	5.00	0.90	22.57	542.63
Min	505.37	110.77	4.00	0.87	21.87	440.22
			Panels ($C_f = 74.92$ kg/m^3)			
Mean	976.18	121.25	5.00	0.83	20.65	758.88
SD	174.51	5.17	1.22	0.04	0.89	147.15
COV (%)	17.88	4.26	24.49	4.31	4.31	19.39
N	5	5	5	5	5	5
Max	1,176.07	126.28	7.00	0.87	21.70	978.13
Min	707.44	115.22	4.00	0.79	19.80	578.39

was applied to compensate for this influence. The procedure is as follows: first, a corrected displacement must be found ($\Delta = 25$ mm $\times k$, $k = 100/\text{h}$); then the corrected energy (E_C) is the energy corresponding to the corrected displacement (E_Δ) multiplied by the factor k ($E_C = E_\Delta \times k$).

From Table 3 the corrected energy absorption results (E_C) are as follows: 397.85 ± 30.31, 494.18 ± 37.12, and 758.88 ± 147.15 J for panels with fiber contents of 33.88, 63.02, and 74.92 kg/m^3, respectively. These results will be used for further analysis in subsequent sections. Similar COVs were found for the two lowest fiber contents. The considerably higher COV observed for specimens with the highest fiber content is probably due to the more pronounced variation in thickness and number of cracks in these panels. Microcraks or internal cracks could also influence differently the COV of tested panels with high and low fiber content. However, the presence of such microcracks was not assessable in the study.

Barcelona Test

Fig. 8 shows the mean load (P) and absorbed energy (E) versus displacement (δ) curves of the cylinders extracted from the panels of each mixture. The curves were considered only from the displacement relative to the peak load reached in the test.

The results of energy absorption by displacement of the extracted cylinders are presented in Table 4. The results are evaluated up to the postpeak displacement of 5.0 mm, following the same criteria of previous studies that assessed the absorbed energy in regular displacements in FRC (Galobardes and Figueiredo 2015; Liu et al. 2018) and SFRSC (Silva 2017; Galobardes et al. 2019) through the BCN test.

The load results are not considered in the analysis since they are not part of the study. The mean values, SD, COV, sample size (N), and maximum (max) and minimum (min) values are presented in Table 4.

(a) (b)

Fig. 7. (a) Typical crack pattern including four major cracks for medium and lower fiber contents; and (b) multiple cracks observed in panel with highest energy absorption for higher fiber contents.

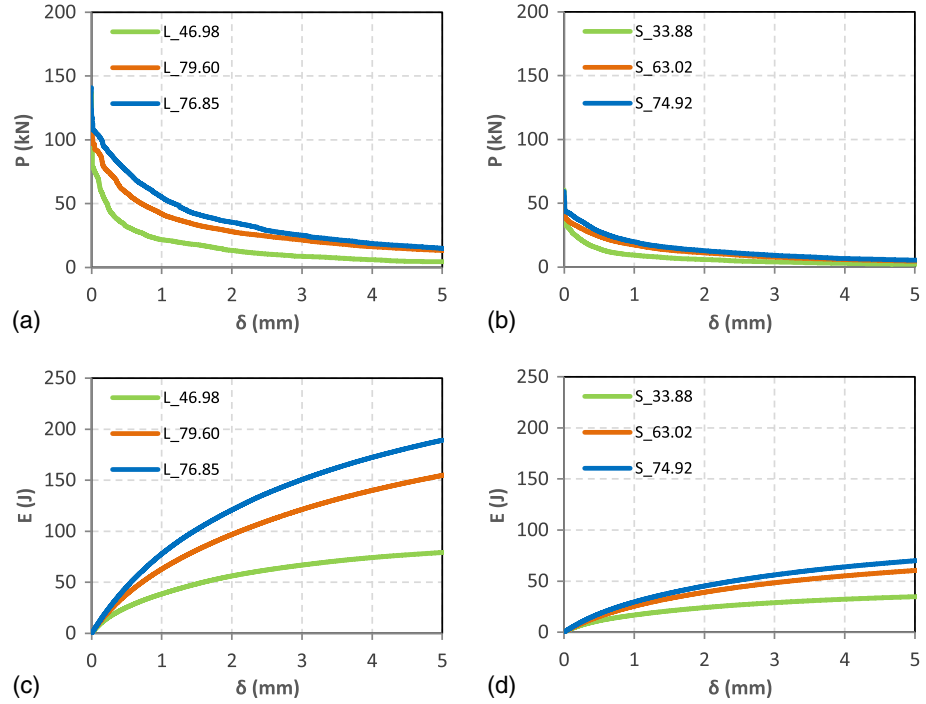

Fig. 8. Average curves of load by displacement in cylinders of (a) Ø150 × 150 mm (fiber contents of 46.98, 79.60, and 76.85 kg/m^3); and (b) Ø100 × 100 mm (fiber contents of 33.88, 63.02, and 74.92 kg/m^3); and of energy absorption by displacement in cylinders of (c) Ø150 × 150 mm; and (d) Ø100 × 100 mm by BCN test.

Table 4. Absorbed energy in 5.0 mm (E_5) in Joules, for cylinders of Ø150 × 150 mm and Ø100 × 100 mm, based on BCN test

	Cylinders of Ø150 × 150 mm				Cylinders of Ø100 × 100 mm		
C_f (kg/m^3)	46.98	79.60	76.85	C_f (kg/m^3)	33.88	63.02	74.92
Mean	79.07	154.67	189.24	Mean	34.18	60.35	69.91
SD	17.61	26.64	39.81	SD	12.36	16.41	15.04
COV (%)	22.27	17.22	21.04	COV (%)	36.17	27.18	21.51
N	6	6	6	N	23	30	30
Max	92.65	186.08	241.24	Max	54.52	86.12	102.06
Min	52.27	118.93	129.54	Min	16.08	22.69	40.98

Table 4 analysis of the energy absorption results of the large cylinders in the displacement of 5 mm shows the following absorbed energies, in increasing order: 79.07 ± 17.61, 154.67 ± 26.64, and 189.24 ± 39.81 J for cylinders with fiber contents of 46.98, 79.60, and 76.85 kg/m^3, respectively. It is observed that the cylinders with fiber content of 76.85 kg/m^3 show a higher level of energy absorption in relation to the cylinders of 79.60 kg/m^3, despite having lower fiber content. This may also be due to a better orientation in relation to the crack surface which may occurs randomly.

Analysis of the average absorption results of the small cylinders shows the following absorbed energies at 5 mm: 34.18 ± 12.36, 60.35 ± 16.41, and 69.91 ± 15.04 J for cylinders with fiber contents of 33.88, 63.02, and 74.92 kg/m^3, respectively. The increasing order in energy absorption is related to the fiber content. The COVs were generally higher for the small cylinders, following the trend observed in the fiber content, as expected and as discussed in more depth in the next section.

Comparison of Coefficients of Variation

Fig. 9 shows the COVs of the energy absorption results obtained from the square panel tests EN 14488-5 (Table 3) and BCN tests (Table 4). It can be seen that the higher COVs correspond to the small cylinders of the BCN test, with a mean COV of 28.29%. In an intermediate situation are the large cylinders of the BCN test, with a mean COV of 20.18%. The panels have the smallest variation, with a mean COV of 11.51%.

In general, the COV of the absorbed energies is higher for small specimens. The COVs obtained with small cylinders were higher than those of the large ones, although they have a lower amplitude of results. A similar trend was found by Aire et al. (2013), who evaluated the FRC in different sizes of cylinders using the BCN test. This behavior can also be associated with the size of the specimen that defines the area of the fractured section. The larger this area, the smaller the COV, as observed in the study by Cavalaro and Aguado (2015). In addition, in the small cylinders, the COVs decrease since the fiber content increases, while in the large cylinders it remains practically constant in all mixtures. These facts show that the large cylinders maintain a more stable behavior during the BCN test.

The COVs obtained in the EN 14488-5 panel tests were lower than those obtained in the BCN tests for each mixture. This may be due to a larger fracture surface. Similarly, it may be due to the fact that great care was taken before the test with placing metal plates to ensure continuous contact between the panels and the support and

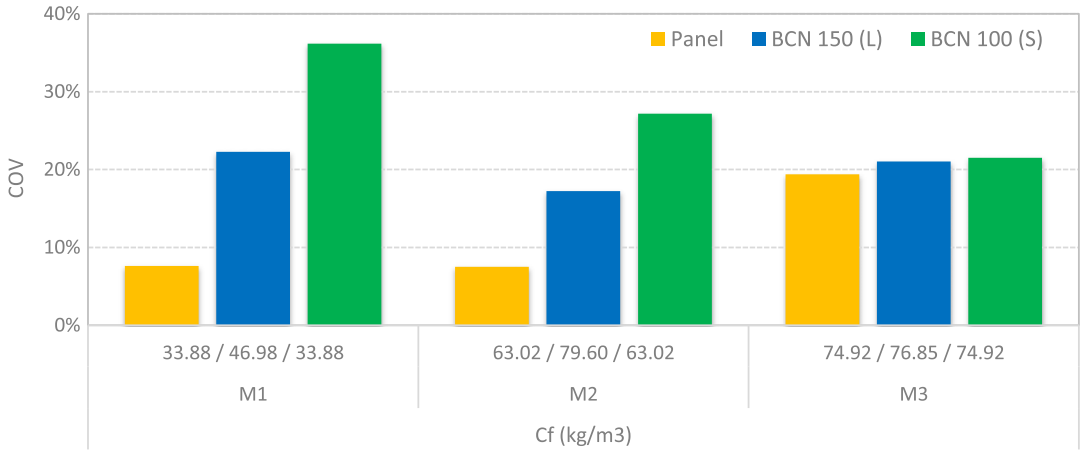

Fig. 9. Comparison of COVs of energy absorption results of EN 14488-5 test and BCN tests.

during spraying so as to avoid buckling on the panels. Several authors have reported that the COV decreases with enhancements to the fracture surface (Carmona et al. 2018). Nonetheless, the COV increases in the mixture with higher fiber content. This may be due to the fact that panels of 74.92 kg/m^3, besides having a higher fiber content, show the greatest variation in thickness and number of cracks, resulting in a greater variation of energy absorption results.

Mix Design Correlations and Comparative Analysis

Comparative analysis of the absorbed energy of the SFRSC is based on the analysis of mix design correlations. These correlations are focused on the average energy absorption results between the square panel tests EN 14488-5 and BCN tests (Tables 3 and 4, respectively). The resulting R^2 values for the correlations between the square panel test EN 14488-5 and BCN tests on small and large cylinders are similar, with values of 0.9809 and 0.9798, respectively (Fig. 10). The good correlations indicate that any of the cylinders can be used in the evaluation of the energy absorption of the SFRSC, replacing the panels.

The comparative analysis is also based on the correlation of the energy absorption results of the square panel test EN 14488-5 and BCN tests on both sizes of cylinders with fiber content in each evaluated element (individual results that generated Tables 2–4). These correlations are shown in Fig. 11(a). The best correlation corresponds to the square panel test ($R^2 = 0.9714$), with a sample size of 14 panels. The correlations obtained in the BCN tests on small and large cylinders were 0.9538 and 0.9568, with sample sizes of 83 and 18 cylinders, respectively.

The experimental design generated the difference in the number of parameter points of the tests in the linear fittings in Fig. 11. In the case of the square panel test, the sample type and number respond to those typically adopted for the quality control of shotcrete. Since the BCN is an alternative test without the support of specific standards for shotcrete, the number of specimens was increased to evaluate the significance of the test variability.

To further verify the correspondence between the test methods, the absorbed energy results were divided by the crack area of each specimen tested. In the BCN tests, the absorbed energy was divided by the area of the rectangle that forms the cylinder, multiplied by

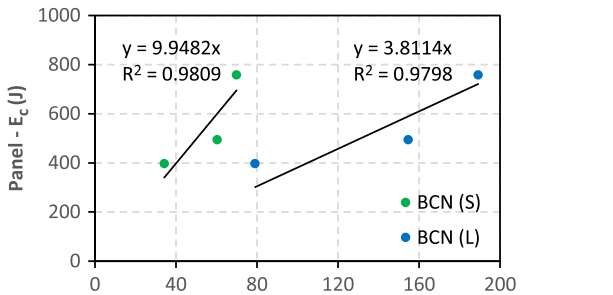

Fig. 10. Correlation of average energy absorption results between the square panel test EN 14488-5 and BCN tests.

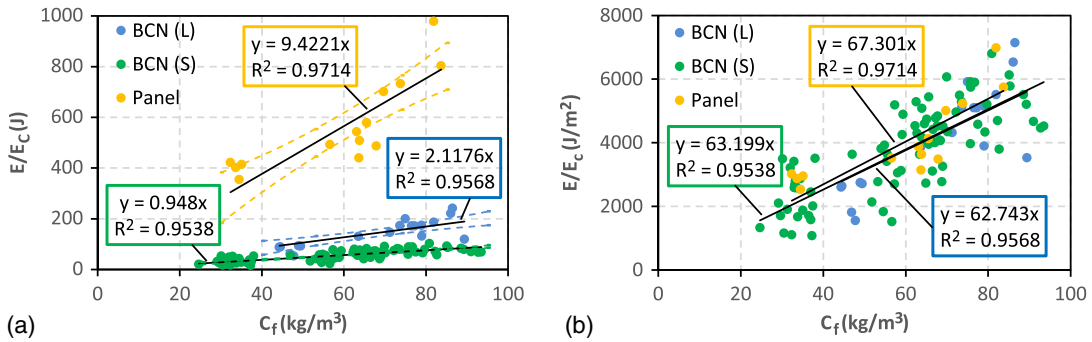

Fig. 11. Correlation between energy absorption results from the square panel test EN 14488-5 and BCN tests with fiber content, in (a) J–kg/m^3; and (b) J/m^2–kg/m^3.

Table 5. Correlation for energy levels required by EN 14487-1 (CEN 2005) and BCN tests [$E_{Panel,25}$ and $E_{BCN,5.0}$, δ (mm)] in Joules, and average fiber content C_f in kilograms per cubic meter

EN 14487-1	EN 14488-5	BCN (L)	BCN (S)	Fiber content
Class	E_{25}	$E_{5.0}$	$E_{5.0}$	C_f
E 500	500 (±54)	112 (±19)	50 (±2)	53
E 700	700 (±68)	157 (±15)	70 (±3)	74
E 1,000	1,000 (±148)	224 (±36)	100 (±7)	106

three, since this is the number of cracks that commonly appear in this test (Pujadas 2013). In the panels, the absorbed energy was divided by the cross-sectional area multiplied by two, since the cracking pattern generally consisted of four cross-shaped major cracks. The correlations between energy absorbed per area and fiber content are shown in Fig. 11(b). It can be seen that the three tests have similar trend lines. Grouping them into a single correlation, the trend line equation is $y = 63.584x$, with an R^2 value of 0.9562. This fact reinforces the concept that the tests are correlated with each other. It is also noteworthy that the absorbed energy results have an almost constant range as the fiber content increases.

From Fig. 11(a) it is possible to determine which energy level corresponds to each test for a given fiber content. This can be used to evaluate the SFRSC by the BCN test according to design methods based on square panel tests results, such as the EN 14487-1 (CEN 2005) standard.

According to EN 14487-1, in the square panel test, to evaluate the SFRSC, three energy absorption levels are considered, in 25 mm of displacement. This type of classification can be associated with empirical tunnel sizing methods, which define the application of SFRSC according to the competence of the rock mass (Barton 2002; Concrete Institute of Australia 2010; Rehman et al. 2019). The energy requirements are: class E 500, E 700, and E 1,000 of 500, 700, and 1,000 J, respectively. From Fig. 11(a), the energy absorption levels of the BCN test, on large and small cylinders, that correspond to these energy requirements and the average fiber content to achieve these energies, are shown in Table 5. Because all regressions in Fig. 11(a) are linear, there may be a linear relationship between the values obtained. However, specific studies need to be done to obtain correlations of energy absorption with other types of fibers.

The energy requirements for each test and average fiber content were calculated considering the confidence intervals of linear regression, at a 90% confidence level, obtained from individual results that generated Tables 2–4, according to the method of Freund and Simon (2002). The confidence intervals are presented in brackets in Table 5 and are also indicated by dashed lines in Fig. 11(a).

Sample Size Analysis

A very common question for tunnel designers and builders concerns the representative sample size needed to evaluate a structure. For this, based on the results, the reliable sample size was determined using the method of Bussab and Moretin (2002), through Eq. (2), where the statistical values are sample size (n), t-distribution (t) according to the confidence level (α), SD, and acceptable error. In the present case, it was considered an average value according to the COVs evaluated, i.e., 20% of the mean value (e). Table 6 shows a comparison of sample sizes obtained for BCN tests on small and large cylinders and for the square panel test EN 14488-5, according to the results of Tables 3 and 4, respectively

$$n = \frac{\tau^2_{n-1} \cdot s^2}{e^2} \tag{2}$$

Evaluating sample sizes at a 95% confidence level, for the BCN test on large cylinders, the sample is almost constant for all mixtures, ranging from five to nine cylinders. The BCN test on small cylinders requires a larger sample of 15 cylinders for lower fiber content (33.88 kg/m^3). For larger fiber contents (63.02 and 74.92 kg/m^3) the sample decreases to eight and five cylinders, respectively. In the case of the square panel test, only two samples are required for mixtures of 33.88 and 63.02 kg/m^3. However, for the mixture with higher fiber content (74.92 kg/m^3), eight panels are required. The increase in the number of specimens required for the EN 14488-5 test with the highest fiber content was due to the increase in the COV of this series, which was generated by the variation of panel thickness and number of cracks. This tendency of increasing number of specimens associated with the highest fiber content was not especially evident for the BCN tests that presented higher uniformity on geometry and crack pattern characteristics.

This high number of specimens can also be attributed to the fact that the fiber used has a low aspect ratio. As a result, the reinforcement capacity is more susceptible to variations in the number of fibers present in the cracking area. Therefore, this evaluation can be considered critical, and the number of specimens indicated must meet the confidence level for sprayed concretes reinforced with fiber with a higher aspect ratio. Considering that the number of specimens in the sample was shown to be below the desired number for a few test conditions, the findings represent a valid contribution to the literature.

Although cylinders for the BCN tests require a larger number of samples, they are easily handled and transported, as a small cylinder weighs around 2 kg and a large one 6.5 kg, much less than the small panels for the square panel test, which weighs around 110 kg. This fact would noticeably improve the technology control process both on site and in the laboratory, in addition to having the advantage of being able to extract cores directly from the structure in different locations. However, in cases where existing structures are being evaluated, it may be necessary to extract a larger number of specimens to obtain representative results.

Conclusions

This study showed a possible correlation between the results obtained on energy absorption in BCN tests in small and large extracted cylinders and the square panel test EN 14488-5. The main conclusions were as follows:

- The level of energy absorption is directly related to the actual fiber content of the SFRSC, which makes it possible to determine

Table 6. Sample size (n) according to the statistical measurement values

$1-\alpha$	90%	95%	$1-\alpha$	90%	95%	$1-\alpha$	90%	95%
C_f (kg/m^3)	BCN (L)		C_f (kg/m^3)	BCN (S)		C_f (kg/m^3)	EN 14488-5	
46.98	6	9	33.88	10	15	33.88	1	2
79.60	4	5	63.02	6	8	63.02	1	2
76.85	5	8	74.92	4	5	74.92	5	8

which energy level corresponds to each test for a given fiber content. When the energy absorption is divided by the fracture area observed in the specimens of each test, they maintain the same trend line, showing the correspondency between all tests.

- The COV of energy absorption associated with the small cylinders is higher than those of the large ones. In the small cylinders, the COVs decrease since the fiber content is enhanced, while in the large cylinders it remains almost constant. This shows that the large cylinders provide more uniform results in the BCN tests due to the larger crack area. The panel tests have the smallest COV, which could be associated with the even larger fracture surface. However, the COV increases at higher fiber contents because of variations in the number of cracks together with the panel thickness in this particular case. Thus, specimens for this type of test should be produced with care to minimize the variation of their final thickness.
- The largest COV of the BCN test is clearly disadvantageous for obtaining representative results. Nonetheless, the BCN test can be used for routine control and especially for existing SFRSC structure evaluation once it becomes possible to perform the test with extracted cores. Also, the BCN test has the advantage of using smaller equipment and smaller specimens, which creates much better working conditions for operators in the laboratory.
- The good correlations of the absorbed energy results of the square panel test and BCN test in extracted cylinders justify the use of any of the cylinders in the evaluation of the absorbed energy of the SFRSC. The BCN test can be considered representative in terms of evaluating the values of absorbed energy in underground works of SFRSC, as long as the correspondence of absorbed energy is established from previous studies.
- Cylindrical cores can be extracted in situ, making it possible to evaluate actual tunnel lining conditions. The fact that specimens can be used for two determinations (fiber content effectively incorporated into the structure and the mechanical behavior of the SFRSC) expands the quality control potential of the tunnel lining construction, providing greater reliability in the process. However, the obtained correlations could not be extrapolated and, as a consequence, they must be determined for each project in the previous qualification studies of the SFRSC.

Data Availability Statement

All data, models, and code generated or used during the study appear in the published article.

Acknowledgments

The authors gratefully acknowledge the support of P&D ANEEL (Pesquisa e Desenvolvimento—Agencia Nacional de Energia Eletrica, Brasil) and Brazilian companies CPB (Concreto Projetado Brasil), Solotrat Engenharia, and Holcim Brasil. The first and third authors would like to thank the National Council for Scientific and Technological Development (Conselho Nacional de Desenvolvimento Científico e Tecnológico–CNPq, Brasil) for the support provided through the doctoral scholarship and financial resources provide by the research project (Proc. No. 305055/2019-4).

References

ABNT (Associação Brasileira Normas Técnicas). 2007. *Fibras de aço para concreto—Especificações*. ABNT NBR 15530. Rio de Janeiro, Brazil: ABNT.

AENOR (Asociación Española de Normalización y Certificación). 2010. *Hormigones con fibras. Determinación de la resistencia a fisuración, tenacidad y resistencia residual a tracción. Método Barcelona*. UNE 83515. Madrid, Spain: AENOR.

Aire, C., C. Molins, and A. Aguado. 2013. "Ensayo de doble punzonamiento para concreto reforzado con fibra: Efecto del tamaño y origen de la probeta." [In Spanish.] *Concreto y Cemento. Investigación y Desarrollo* 5 (1): 17–31.

Armelin, H. S., and N. Banthia. 2002. "A novel double anchored steel fiber for shotcrete." *Can. J. Civ. Eng.* 29 (1): 58–63. https://doi.org/10.1139/l01-080.

ASTM. 2012. *Standard test method for flexural thoughness of fiber reinforced concrete (using centrally loaded round panel)*. ASTM C1550-12. West Conshohocken, PA: ASTM.

Austin, S. A., C. H. Peaston, and P. J. Robins. 1997. "Material and fibre losses with fibre reinforced sprayed concrete." *Constr. Build. Mater.* 11 (5–6): 291–298. https://doi.org/10.1016/S0950-0618(97)00050-0.

Banthia, N., J.-F. Trottier, and D. Beaupré. 1994. "Steel-fiber-reinforced wet mix shotcrete: Comparison with cast concrete." *J. Mater. Civ. Eng.* 6 (3): 430–437. https://doi.org/10.1061/(ASCE)0899-1561(1994)6:3(430).

Barton, N. 2002. "Some new Q-value correlations to assist in site characterization and tunnel design." *Int. J. Rock Mech. Min. Sci.* 39 (2): 185–216. https://doi.org/10.1016/S1365-1609(02)00011-4.

Bernard, E. S. 2002. "Correlations in the behaviour of fibre reinforced shotcrete beam and panel specimens." *Mater. Struct.* 35 (3): 156–164. https://doi.org/10.1007/BF02533584.

Bernard, E. S. 2008. "Early-age load resistance of fibre reinforced shotcrete linings." *Tunnelling Underground Space Technol.* 23 (4): 451–460. https://doi.org/10.1016/j.tust.2007.08.002.

Bernard, E. S. 2013. "Development of a 1200-mm-diameter round panel test for post-crack assessment of fiber-reinforced concrete." *Adv. Civ. Eng. Mater.* 2 (1): 457–471. https://doi.org/10.1520/ACEM20120021.

Bernard, E. S., and A. H. Thomas. 2020. "Fibre reinforced sprayed concrete for ground support." *Tunnelling Underground Space Technol.* 99 (1): 103302. https://doi.org/10.1016/j.tust.2020.103302.

Bjøntegaard, Ø. 2009. *Energy absorption capacity for fibre reinforced sprayed concrete. Effect of friction on round and square panel tests whit continuous support (series 4)*. Oslo, Norway: Norwegian Public Roads Administration.

Bussab, W., and P. Moretim. 2002. *Estatística básica*. [In Portuguese.] 5th ed. São Paulo, Brazil: Editora Saraiva.

Carmona, S., C. Molins, and A. Aguado. 2018. "Correlation between bending test and Barcelona tests to determine FRC properties." *Constr. Build. Mater.* 181 (Aug): 673–686. https://doi.org/10.1016/j.conbuildmat.2018.05.253.

Carmona, S., C. Molins, and S. García. 2020. "Application of Barcelona test for controlling energy absorption capacity of FRS in underground mining works." *Constr. Build. Mater.* 246 (Jun): 118458. https://doi.org/10.1016/j.conbuildmat.2020.118458.

Cavalaro, S. H. P., and A. Aguado. 2015. "Intrinsic scatter of FRC: An alternative philosophy to estimate characteristic values." *Mater. Struct.* 48 (11): 3537–3555. https://doi.org/10.1617/s11527-014-0420-6.

Cavalaro, S. H. P., R. López, J. M. Torrents, and A. Aguado. 2015. "Improved assessment of fibre content and orientation with inductive method in SFRC." *Mater. Struct.* 48 (6): 1859–1873. https://doi.org/10.1617/s11527-014-0279-6.

Cavalaro, S. H. P., R. López, J. M. Torrents, A. Aguado, and P. García. 2016. "Assessment of fibre content and 3D profile in cylindrical SFRC specimens." *Mater. Struct.* 49 (1–2): 577–595. https://doi.org/10.1617/s11527-014-0521-2.

CEN (European Standard). 2005. *Sprayed concrete—Part 1: Definitions, specifications and conformity*. EN 14487-1. Brussels, Belgium: CEN.

CEN (European Standard). 2006. *Testing sprayed concrete—Part 5: Determination of energy absorption capacity of fibre reinforced slab specimens*. EN 14488-5. Brussels, Belgium: CEN.

Cengiz, O., and L. Turanli. 2004. "Comparative evaluation of steel mesh, steel fibre and high-performance polypropylene fibre reinforced shotcrete in panel test." *Cem. Concr. Res.* 34 (8): 1357–1364. https://doi.org/10.1016/j.cemconres.2003.12.024.

Chen, L., X. Zhang, and G. Liu. 2020. “Analysis of dynamic mechanical porperties of sprayed fiber-reinforced concrete based on the energy conversion principle.” *Constr. Build. Mater.* 254 (Sep): 119167. https://doi.org/10.1016/j.conbuildmat.2020.119167.

Concrete Institute of Australia. 2010. *Shotcreting in Australia: Recommended practice*. 2nd ed. Sydney, Austrilia: Concrete Institute of Australia.

EFNARC (European Federation of Producers and Applicators of Specialist Products for Structure). 1996. *European specification for sprayed concrete*. Hampshire, UK: EFNARC.

EFNARC (European Federation of Producers and Applicators of Specialist Products for Structure). 2011. *Testing sprayed concrete. EFNARC three point bending test on square panel with notch*. Hampshire, UK: EFNARC.

Figueiredo, A. D. 1997. “Parâmetros de controle e dosagem do concreto projetado com fibras de aço.” [In Portuguese.] Thesis (Doctorate). Dept. of Civil Construction Engineering, Univ. of São Paulo.

Figueiredo, A. D., and P. R. L. Helene. 1993. “Reflexões sobre a reflexão.” [In Portuguese.] *Téchne-Revista de Tecnologia da Construção* 5: 24–27.

Freund, J. E., and G. A. Simon. 2002. *Estatística aplicada. Economia, administração e contabilidade*, [In Portuguese.] 9th ed. Porto Alegre, Brazil: Bookman.

Galobardes, I., and A. D. Figueiredo. 2015. “Correlation between beam and Barcelona tests for FRC quality control for structural application.” In *Proc., 8th Int. Conf. Fibre Concrete 2015*. September 10–11. Prague, Czech Republic: Czech Technical University.

Galobardes, I., C. S. Silva, A. D. Figueiredo, S. H. P. Cavalaro, and C. I. Goodier. 2019. “Alternative control of steel fibre reinforced sprayed concrete (SFRSC).” *Constr. Build. Mater.* 223 (Oct): 1008–1015. https://doi.org/10.1016/j.conbuildmat.2019.08.003.

Ginouse, N., and M. Jolin. 2015. “Investigation of spray pattern in shotcrete applications.” *Constr. Build. Mater.* 93 (Sep): 966–972. https://doi.org/10.1016/j.conbuildmat.2015.05.061.

Jolin, M. 1999. “Mechanisms of placement and stability of dry process shotcrete.” Ph.D. thesis. Dept. of civil engineering, Univ. of British Columbia.

Juhasz, P. K., L. Nagy, and P. Schaul. 2017. “Correlation of the results of the standard beam and EFNARC panel test.” In *Proc., World Tunnel Congress 2017—Surface challenges—Underground Solutions*. Bergen, Norway: International Tunnelling and Underground Space Association.

Kaufmann, J., K. Frech, F. Schuetz, and B. Münch. 2013. “Rebound and orientation of fibers in wet sprayed concrete applications.” *Constr. Build. Mater.* 49 (Dec): 15–22. https://doi.org/10.1016/j.conbuildmat.2013.07.051.

Leung, C. K. Y., R. Lai, and A. Y. F. Lee. 2005. “Properties of wet-mixed fiber reinforced shotcrete and fibre reinforced concrete with similar composition.” *Cem. Concr. Res.* 35 (4): 788–795. https://doi.org/10.1016/j.cemconres.2004.05.033.

Liu, G., W. Cheng, L. Chen, G. Pan, and Z. Liu. 2020. “Rheological properties of fresh concrete and its application on shotcrete.” *Constr. Build. Mater.* 243: 118180. https://doi.org/10.1016/j.conbuildmat.2020.118180.

Liu, X., M. Yan, I. Galobardes, and K. Sikora. 2018. “Assessing the potential of functionally graded concrete using fibre reinforced and recycled aggregate concrete.” *Constr. Build. Mater.* 171: 793–801. https://doi.org/10.1016/j.conbuildmat.2018.03.202.

Monte, R., G. S. Toaldo, and A. D. Figueiredo. 2014. “Avaliação da tenacidade de concretos reforçados com fibras através de ensaios com sistema aberto.” [In Portuguese.] *Matéria (Rio Janeiro)* 19 (2): 132–149. https://doi.org/10.1590/S1517-70762014000200008.

Myren, S. A., and Ø. Bjøntegaard. 2010. “Round and square panel tests—A comparative study.” In *Shotcrete: Elements of a system*. London: Taylor & Francis.

Papworth, F. 2002. “Design guidelines for the use of fibre reinforced sprayed concrete in ground support.” In *Proc., 27th Conf. on Our World in Concrete & Structures*. August 29–30, 2002. Singapore: CI-Premier PTE.

Pfeuffer, M., and W. Kusterle. 2001. “Rheology and rebpund behaviour of dry-mix shotcrete.” *Cem. Concr. Res.* 31 (11): 1619–1625. https://doi.org/10.1016/S0008-8846(01)00614-7.

Pujadas, P. 2013. “Caracterización y diseño del hormigón reforzado con fibras plásticas.” [In Spanish.] Thesis doctoral, Dept. of Civil and Environmental Engineering, Polytechnic Univ. of Catalonia.

Pujadas, P., A. Blanco, S. H. P. Cavalaro, A. de la Fuente, and A. Aguado. 2013. “New analytical model to generalize the Barcelona test using axial displacement.” *J. Civ. Eng. Manage.* 19 (2): 259–271. https://doi.org/10.3846/13923730.2012.756425.

Rehman, H., A. M. Naji, J. J. Kim, and H. Yoo. 2019. “Extension of tunneling quality index and rock mass rating systems for tunnel support design through back calculations in highly stressed jointed rock mass: An empirical approach based on tunneling data from Himalaya.” *Tunnelling Underground Space Technol.* 85 (Mar): 29–42. https://doi.org/10.1016/j.tust.2018.11.050.

Salehian, H., J. A. O. Barros, and M. Taheri. 2014. “Evaluation of the influence of post-cracking response of steel fibre reinforced concrete (SFRC) on load carrying capacity of SFRC panels.” *Constr. Build. Mater.* 73 (Dec): 289–304. https://doi.org/10.1016/j.conbuildmat.2014.09.043.

Sandbakk, S. 2011. “Fibre reinforced concrete evaluation of test methods and material development.” Doctoral thesis, Dept. of Structural Engineering, Norwegian Univ. of Science and Technology.

Silva, C. L. 2017. “Proposta de metodologia alternativa para controle de qualidade da aplicação estrutural do concreto projetado reforçado com fibras de aço.” [In Portuguese.] Dissertação (Mestrado). Dept. of Civil Construction Engineering, Universidade de São Paulo.

Silva, C. L., I. Galobardes, P. Pujadas, R. Monte, A. D. Figueiredo, S. H. P. Cavalaro, and A. Aguado. 2015. “Assessment of fibre content and orientation in SFRC with the inductive Method. Part 2: Application for the quality control of sprayed concrete.” *J. Nondestr. Test. Ultrason.* 20: 18384.

Simão, L. C. R., A. B. Nogueira, R. Monte, R. P. Salvador, and A. D. Figueiredo. 2019. “Influence of the instability of the double punch test on the post-crack response of fiber-reinforced concrete.” *Constr. Build. Mater.* 217 (Aug): 185–192. https://doi.org/10.1016/j.conbuildmat.2019.05.062.

Thomas, A. 2020. *Sprayed concrete lined tunnels*. 2nd ed. London: Taylor & Francis.

Thorenfeldt, E. 2006. *Fibre reinforced concrete panels. Energy absorption capacity for standard sample*. [In Norwegian.] SINTEF Memo. Oslo, Norway: Norwegian Public Roads Administration.

Torrents, J. M., A. Blanco, P. Pujadas, A. Aguado, P. Juan-García, and M. A. Sánchez-Moragues. 2012. “Inductive method for assessing the amount and orientation of steel fibers in concrete.” *Mater. Struct.* 45 (10): 1577–1592. https://doi.org/10.1617/s11527-012-9858-6.